Desalination and Water Treatment
www.deswater.com
doi: 10.5004/dwt.2023.30030

313 (2023) 331–340
November

Multi-objective decision making study for flood construction risk analysis in civil engineering

Jianhua Zhou

Puyang Vocational and Technical College, Puyang 457000, China, email: 13461766801@163.com

Received 20 August 2023; Accepted 22 October 2023

ABSTRACT

Flood construction risk control occurs throughout the entire civil engineering construction phase and is an important issue that must be considered in engineering planning and design. However, risk analysis requires the coordination of indicators that affect each other in many aspects such as construction duration and potential losses, and there is a lack of corresponding multi-objective decision-making methods. The study takes the construction period of an earth and rock dam as an example, and based on the construction of a mathematical model of flood risk during the construction period of a civil engineering project, the flood risk is calculated through the Monte–Carlo simulation method. The multi-objective decision making model was then constructed by using the improved hierarchical analysis method of kernel entropy weighting to determine the weights of the decision indicators and introducing the approximate ideal solution ranking method to complete the multi-objective decision making model of the diversion scheme during the construction period. The results show that in the Receiver Operating Characteristic Curve area comparison, the proposed method can reach 0.941. In the comprehensive F1 value change, the method gradually stabilises when the time reaches 0.98s, and the F1 value is 98.45%. In the practical application of the reservoir construction project, the method has an inflow accuracy of 96.355% and a running time of 0.182s, indicating that it can effectively avoid risks and is more efficient, providing a new technical reference for the safety of civil engineering flood construction.

Keywords: Civil engineering; Flood construction; Risk analysis; Multi-objective decision making

1. Introduction

With the continuous progress of China's economy and technology, the mechanisation level of civil engineering construction and dam construction technology is getting more and more sophisticated. High-tech high earth engineering buildings and earth and rock dams are being built across the country, which makes civil engineering rock dams have a large development space in the future construction of water conservancy projects [1]. Earth and rock dams are simple in structure, easy to Master's in Construction Technology and convenient in operation and management, and are widely used in the construction of controlled water conservancy projects. In earth and rock dams, due to the material characteristics of concrete, the flood stage during construction is usually achieved by retaining water in the dam body and releasing it in a drainage structure. In contrast to earth and rock dams, the various parameters at this stage do not meet the design requirements and are difficult to resist flooding, which can lead to flooding and even dam failure [2]. At the same time, statistics show that the number one cause of dam failure is flooding, which occurs during the construction phase with a probability of 18%. Under these conditions, not only is the project itself irreparably damaged, but the lives and property of people downstream are also at serious risk. However, in the construction of civil engineering works, earth and rock dams are often overtopped, so in the planning and design of construction works, it is important to analyse the flood risk during the construction phase of civil engineering works, so that construction plans can be made to reduce the risk of construction works [3,4]. At the same time, flood risk during construction provides an important basis for risk control and has become one of the indispensable indicators in the decision-making process for inflow solutions. As a multi-objective complex decision-making problem, the key to the diversion scheme is to coordinate the conflicts between construction cost indicators, risk indicators and schedule indicators. Under the influence of the mutual constraints and incommensurability of the decision indicators, subjective arbitrariness often makes it difficult to maintain a high level of objectivity in the decision-making process [5]. Therefore, in order to cope with this problem, the study proposes to integrate multi-objective decision algorithms with uncertainty analysis to further improve the accuracy and rationality of civil engineering risk analysis for the risk analysis of civil engineering flood construction. The article consists of four main parts. The first part is a review of the literature on multi-objective decision making for civil engineering flood construction risk analysis. The second part is divided into two sections, the first one is on the analysis of civil engineering construction risk during flooding period based on uncertainty analysis, and the second one is on the multi-objective decision making of the inflow solution using TOPSIS. The third section analyses the performance testing and application effects of the multi-objective decision model, and the fourth section summarises the results of the proposed method for multi-objective decision making.

2. Related works

Civil engineering requires both high accuracy and longevity in the construction of water projects, as well as the ability to effectively reduce risk analysis during the construction process. To this end, a fuzzy representation of environmental flows was proposed based on the use of fuzzy theory and eco-hydraulic radii. The results show that following an environmentally friendly operation strategy is beneficial for protecting the environment and improving the overall effectiveness of the reservoir [6]. Bao et al. [7] developed an urban flooding model with uncertain flow in order to prevent urban flooding problems. The experimental results were highly consistent with the flood points of two historical rainstorms in the region. The model can better help to solve the urban flooding problem and improve the solution. He et al. [8] concluded that the stochastic events during the construction process could lead to managers not being able to accurately calculate the energy consumption, duration and benefits of the project, so a multi-objective stochastic optimisation algorithm was proposed to analyse the energy consumption, duration and benefits of the construction process. Experimental results show that the simulation accuracy and the discrimination rate of the benefit values are better than the original algorithm. Feng et al. [9] argue that with the advancement of carbon neutrality research, there is a need for an advanced hydropower energy system that can serve multiple energy sources and through which the system can effectively cope with multiple forms of energy fluctuations. It is also hoped that the system will be able to flexibly regulate various renewable energy sources to improve power system security and stability. Various valuable research directions are proposed in this topic. Nematollahi et al. [10] proposed an MCDM optimisation model for the optimal design of a reservoir system under flood conditions in order to fill in during floods, based on hybrid modelling of a coupled MCDM and an optimisation model of the reservoir and its outlet. The experimental results show that the proposed optimisation model can provide more reasonable recommendations for the design of reservoir outlets.

At the same time, scholars have turned their attention to a variety of approaches to water resources allocation, with Wu et al. [11] proposing an integrated water allocation model that combines social, economic and environmental objectives. The model was used to calculate a water allocation scenario for a particular region, which was analysed independently in terms of demand and supply, and was found to be reasonable and conducive to the development of the region. Mohanavelu et al. [12] compared six different state-of-the-art modelling techniques for a reservoir in order to find a better solution for the operation of the reservoir. The results obtained by the different methods were combined to derive a set of Pareto optimal solutions. After the analysis and comparison, it was finally found that the best operational solution could be derived using deterministic dynamic programming techniques, followed by sampling stochastic dynamic programming and model predictive control. Raseman et al. [13] proposed a new decision framework for optimising water treatment plant operations in order to help water company managers make better decisions. The framework is able to give more optimal decision options based on the decision maker's preference for cost and risk and the specific situation of the water resource. Experimental results show that the framework is effective in helping water company decision makers to make decisions. A multi-objective planning model is presented by Modibbo et al. [14]. Using Nigeria as an example, the researchers used the model to analyse the socio-economic, environmental and energy sectors in Nigeria. The experimental results were shown to be mathematically sound. At the same time, the researchers say the model can be applied to other countries in different contexts. The model can help governments to make sound development strategies.

From the above research by domestic and international scholars, it is clear that the construction of civil engineering has now received the attention of a wide range of scholars. Most of these scholars have used traditional methods around hydropower construction, and few studies have applied machine learning algorithms to civil engineering construction to solve problems such as flood risk analysis in the construction process. In view of this, the study proposes a multi-objective decision-based approach to civil engineering flood construction risk analysis, which is expected to effectively improve the accuracy of risk analysis for civil engineering construction and maintain the safety of water conservancy construction.

3. Methodological design of multi-objective decision making in civil engineering flood construction risk analysis

China is very rich in hydro energy resources and numerous water conservancy projects have been constructed in order to make effective use of water resources. The risk analysis and construction decision scheme in project construction has not been the most effective solution, for this reason the experiment proposes a multi-objective decision-based approach to civil engineering flood construction risk analysis.

3.1. Flood risk analysis for civil engineering construction based on uncertainty analysis

The hydraulic engineering sector has always been concerned with the risk analysis of construction flooding in the civil engineering construction process, which is directly related to the safety of engineering construction and the construction investment and duration of the main project, and is also the basic premise for determining the construction diversion scheme. In civil engineering, the construction of earth and rock dams, for example, can be divided into three stages: initial, medium and late inflow [15,16]. As a whole, flood risk is present throughout the entire construction phase of a civil engineering project. The framework of the risk analysis system is shown in Fig. 1.

In order to avoid serious economic losses and casualties, the probability of flooding is used as a measure of flood risk during the construction phase of a civil engineering project. The mathematical model of flood risk during the construction phase of the civil engineering works is based on the assumption that the diversion phase of the civil engineering works spans over N flooding periods, and is based on certain diversion criteria and the setting of diversion holes.

$$\begin{cases} R_j = P\left(Z(t) \geq H_r \middle| T_H, S_D\right) / T_r \qquad j = 1,2,\cdots,N \\ R = 1 - \prod_{j=1}^{N}\left(1 - R_j\right) \end{cases} \tag{1}$$

where R_j indicates the flood risk for the first j flood period during the construction period of the civil engineering dam; T_H indicates the start of the main flood period, calculated from the results of the stepwise diversion design flood; $Z(t)$ indicates the flood level of the upstream flood at the current time under the design diversion standard; H_r indicates the flood control elevation of the water retaining structures at the current time; S_D indicates the design parameters for the diversion cavern, which include the cavern width B and the cavern height H; T_r indicates the experimentally designed diversion standard; indicates the combined flood risk for the construction period of the civil engineering dam. R indicates the combined flood risk during construction of civil engineering dams. The risk during construction flooding of civil engineering dams is determined by the uncertainty of the relationship between the upstream flood level and the flood control elevation that can be achieved by the dam [17]. A simulation of the flooding environment is shown in Fig. 2.

The calculation of the main uncertainties affecting flood risk in a flooded environment is shown in Eq. (2).

$$R = f\left(Q, q, F(Z), t_r\right) \tag{2}$$

where $F(Z)$ indicates the relationship between the water level and the reservoir area before the uncertainty is mainly caused by the combination of sedimentation, slope collapse in the reservoir area and the error existing in the field survey. Q indicates the upstream incoming flood process; q indicates the discharge capacity of the diversion and discharge structure; t_r indicates the actual work experience time for the dam works to complete the planned filling height. Considering the small probability of the above scenarios occurring during the construction of the dam and the current survey technology, the study focuses on the uncertainties of Q, q and t_r. The corresponding calculations are shown in Eq. (3).

$$\begin{cases} q = \dfrac{A}{\sqrt{1 + \sum \zeta + {2gn^2 l}/{R^{2/3}}}} \sqrt{2g\left(H_0 + il - \eta d\right)} \\ t_r = t_p + \sum_{l=1}^{m} t_l i_l \end{cases} \tag{3}$$

where A indicates the cross-sectional area of the diversion tunnel; $\sum \zeta$ indicates the sum of the local loss factors for

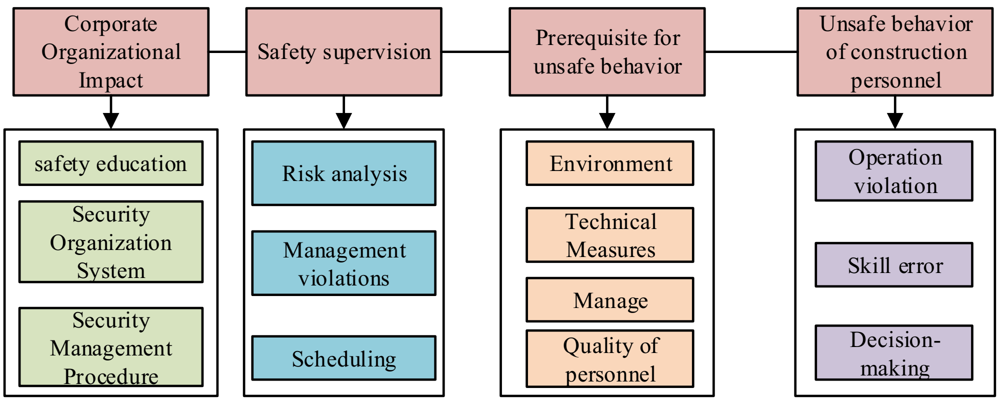

Fig. 1. Framework of the risk analysis system.

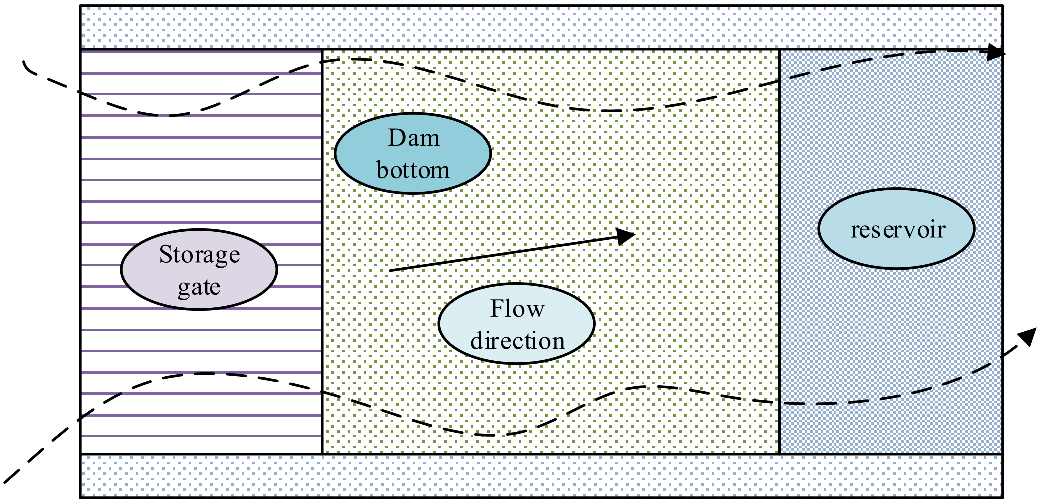

Fig. 2. Simulation of the flood water inlet environment.

the inlet, intermediate and outlet sections; n indicates the roughness factor; l indicates the tunnel length; R indicates the tunnel hydraulic radius; H_0 indicates the water depth above the tunnel inlet floor; i indicates the tunnel bottom slope; η indicates the head ratio at the outlet of the pressurised flow; and d indicates the height of the tank. md indicates the magnitude of the fluctuation in uncertainty caused by the risk factor on the working calendar; d indicates the coefficient of variation, that is, the uncertainty in the occurrence of the risk factor. There are a number of methods for calculating flood risk, the main ones being the recurrence period method, the direct integration method, the mean first order moment method and the Monte–Carlo simulation method [18,19]. The flood risk during the construction period of a civil engineering dam is calculated by taking into account the process of upstream flooding, the discharge capacity of the diversion structure and the uncertainty of the construction schedule. The flood flow simulation is shown in Fig. 3.

The Monte–Carlo method was chosen to calculate the flood risk during the construction period of a civil engineering embankment, as traditional methods are more difficult to solve for the more complex multiple integrals in construction engineering. The distribution of uncertainties and related parameters are first entered, and then the minimum number of simulations to meet the accuracy requirements is determined N_j, calculated in Eq. (4).

$$N_j = \frac{U^2}{\xi^2 T_r}\left(1 - \frac{1}{T_r}\right) \tag{4}$$

where U represents the allowable error in flood risk and T_r represents the experimentally designed inflow criterion. The joint distribution of the flood peak Q and the flood volume W is then constructed as a two-dimensional function, given the designed inflow criterion $T^U(q,w)$. The joint probability density function of $f(q,w)Q$ and W is transformed into a single-valued continuous function of the flood peak Q. Finally, the surface density function is constructed and a certain confidence level is chosen to determine the boundary points of the recurrence period contour. A random number

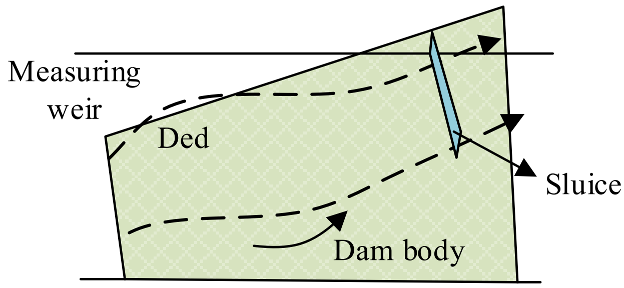

Fig. 3. Simulation of flooding environment.

obeying a uniform distribution between [0,1] is obtained by calculation r_1. If $u = r_1$ is set, then the design value of the flood flow is $q = F_Q^{-1}(u)$ and is checked to see if it satisfies $q_B \le q \le q_C$. If it does, the recurrence period contour can be used to determine the value of v. The corresponding typical flood process is then scaled up using the variable ratio method, as calculated in Eq. (5).

$$\begin{cases} v = \exp\left\{-\left[-\ln\left(1-\frac{1}{T^U}\right)^{\theta} - \left(-\ln u\right)^{\theta}\right]^{1/\theta}\right\} \\ Q(t) = \left(Q_D(t) - Q_{D\max}\right) \times \left(w/T - q\right)\left(W_D/T - Q_{D\max}\right) + q \end{cases} \tag{5}$$

where $Q(t)$ and $Q_D(t)$ represent the flow rate at the time of the incoming flood at t for the simulated and measured floods, respectively; $Q_{D\max}$ represents the peak flow rate of the measured typical flood; W_D represents the flood volume at the time of the measured typical flood at T. The calculation gives a random number that satisfies a uniform distribution between the interval [0,1] r_2. The capacity of the diversion structure under the influence of underwater uncertainties is simulated according to a triangular distribution. The simulation process to obtain the flood control elevation based on the Monte–Carlo method is shown in Fig. 4.

Based on the continuous calculations in Fig. 4 and after several sampling and simulation calculations, the number

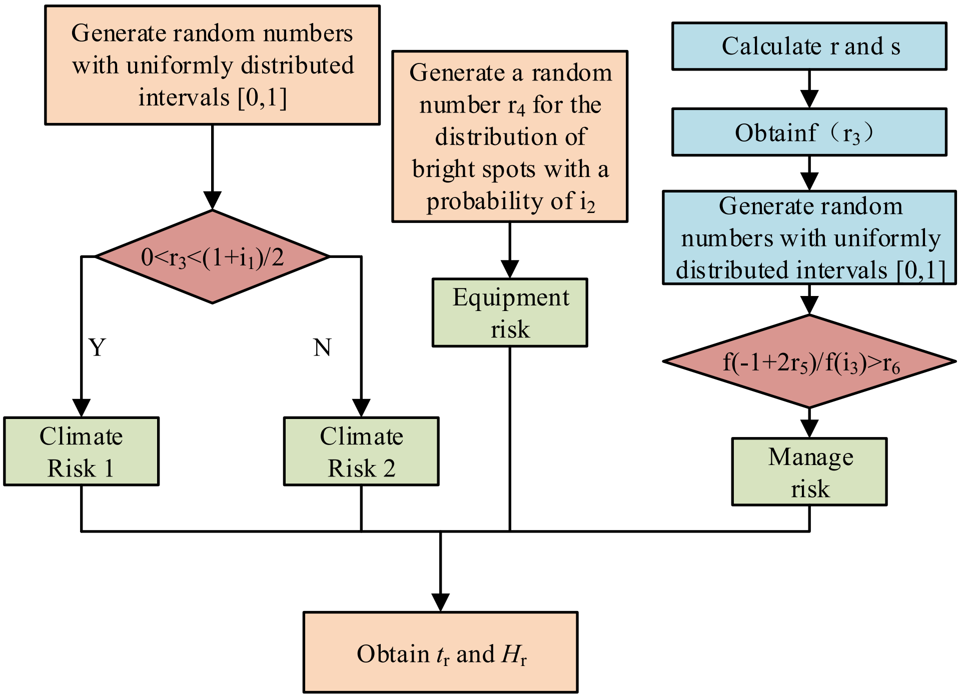

Fig. 4. Flowchart of the method-based flood elevation simulation for civil engineering.

of times for $Z(t) \geq H_r$ was counted and recorded as M_j. The flood risk for the civil engineering construction in the j calculation cycle is calculated and based on this the flood risk for the different inflow stages k and the entire construction period is calculated, Eq. (6).

$$\begin{cases} R_j = \dfrac{M_j}{N_j} \\ R_k = 1 - \prod_{j=x}^{y}\left(1 - R_j\right) \\ R = 1 - \prod_{j=1}^{T}\left(1 - R_j\right) \end{cases} \tag{6}$$

where x,y is the first and last calculation period of the inflow phase, respectively, and kT is the calculation period of the entire construction period of the civil engineering construction.

3.2. Multi-objective decision making for construction diversion schemes based on TOPSIS method

After an effective analysis of the risks of civil engineering construction, the study then goes on to analyse the construction infusion in engineering construction. Different civil engineering constructions have different characteristics, so choosing an effective construction infusion solution is a more complex decision problem [20]. The risk analysis and construction period optimisation process is shown in Fig. 5.

The conflicting relationships between different indicators in the decision-making process for the construction inflow solution necessitates an effective multi-objective decision making process for the construction inflow solution. The study selects the deterministic investment in the inflow building, the risk of failure of the inflow system and the average construction intensity of the inflow building to make an effective decision on the inflow solution in civil engineering construction. The deterministic investment in the inflow structure is directly related to the size of the inflow structure. The calculation is expressed in Eq. (7).

$$C_d = C_{d1} + C_{d2} + C_{d3} + C_{d4} \tag{7}$$

where C_d represents the total deterministic investment in the diversion structure; C_{d1} represents the investment in the diversion and drainage structure; C_{d2} represents the investment in the construction of the upstream weir; C_{d3} represents the investment in the construction of the downstream weir; C_{d4} represents the cost of excavation and pumping of the foundation pit. In general, civil engineering works will be constructed with appropriate emergency plans for flood prevention and rescue to ensure maximum protection of people's lives and safety downstream. The study does not count the losses and risks downstream after the dam collapse, but only the losses caused in the cofferdam pit. The risk loss calculation for the failure of the diversion system obtained is shown in Eq. (8).

$$C_r = \sum_{n=1}^{k}\left(C_{r1} + C_{r2} + C_{r3} + C_{r4} + C_{r5}\right) R_n \left(1 + i\right)^{-n} \tag{8}$$

where C_r represents the total risk loss if the diversion system fails; C_{r1} represents the cost of repairing the upstream and downstream weir failure after the breach; C_{r2} represents the cost of repairing the dam failure; C_{r3} represents the cost

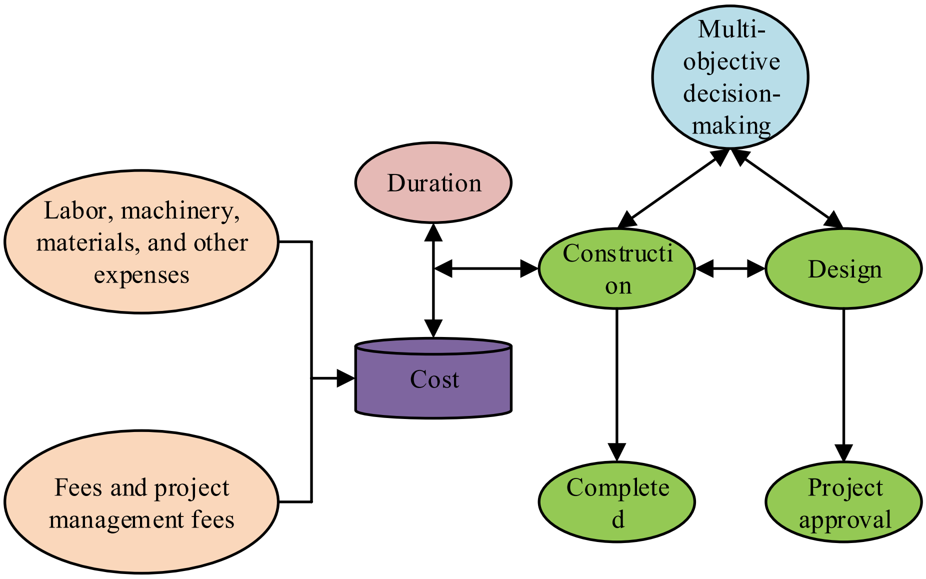

Fig. 5. Risk analysis and construction period optimisation process.

of re-pumping the pit; C_{r4} represents the cost of dredging the pit; C_{r5} represents the loss of machinery and equipment not evacuated from the pit in time; k represents the service life of the weir; i represents the investment of converting the risk loss to the project. The probability calculation gives the discount rate for the base year. The average construction strength of the cofferdam is calculated in Eq. (9).

$$D_d = \frac{V_d}{T_d} \tag{9}$$

where D_d represents the average construction intensity of the cofferdam; V_d represents the amount of work to be done to fill the cofferdam; T_d represents the duration of time to fill the cofferdam. In the multi-objective decision problem, there are many different types and numbers of decision indicators, and different indicators have different degrees of influence on the decision results. After comparing different assignment methods, the experiments choose the improved hierarchical analysis method, the improved entropy method and the combined assignment to calculate the weights of the subjective and objective decision indicators, and determine the weights of different indicators in the inflow scheme by multiplying the combined assignment. The expression of the calculation of the subjective and objective factors is shown in Eq. (10).

$$\begin{cases} \omega_{j_s} = \dfrac{\sqrt[n]{\prod a_{ij}}}{\sum_{j=1}^{n} \sqrt[n]{\prod a_{ij}}} \quad j = 1,2,\cdots,n \\ \omega_{j_o} = \dfrac{\sum_{k=1}^{n} H_k + 1 - 2H_j}{\sum_{l=1}^{n} \left(\sum_{k=1}^{n} H_k + 1 - 2H_j \right)} \end{cases} \tag{10}$$

where ω_{j_s} and ω_{j_o} denote the subjective and objective weights of all indicators, respectively. n denotes the root of the n square. H_k and H_j denote the entropy values of the k and j decision indicators, respectively. The combination of the subjective and objective weights is then used to obtain the new weights ω_j and the resulting multi-objective decisions are used as the final weights. The specific calculation is shown in Eq. (11).

$$\omega_j = \frac{\omega_{j_s}^{\theta} \omega_{j_o}^{1-\theta}}{\sum_{j=1}^{n} \omega_{j_s}^{\theta} \omega_{j_o}^{1-\theta}} \tag{11}$$

where θ represents the preference index of subjective and objective weights, which takes values in the range of $0 \le \theta \le 1$; the smaller the value of θ, the more objective entropy weights the final weights are, and the larger the value of θ, the more subjective weights the final weights are. The TOPSIS method is simpler to operate and provides a clearer representation of the gap between different decision options. In view of this, the TOPSIS method was used to make a multi-objective decision on the construction diversion scheme in civil engineering construction. The selection of the construction and investment of the diversion project, the loss of risk of failure of the diversion system and the average construction strength of the cofferdam are first carried out. An indicator matrix $Y = (y_{ij})_{m3}$ was created using the m diversion options from the alternatives [Eq. (12)].

$$Y = \left(y_{ij} \right)_{m3} = \begin{bmatrix} y_{11} & y_{12} & y_{13} \\ y_{21} & y_{22} & y_{23} \\ \vdots & \vdots & \vdots \\ y_{m1} & y_{m2} & y_{m3} \end{bmatrix} \tag{12}$$

where y_{ij} (i = 1, 2, L, m, j = 1, 2, 3) represents the value of the j indicator for the i scenario. The decision indicators for the inflow scenarios are then standardised and the indicator matrix $Y = (y_{ij})_{m.3}$ is transformed into a new dimensionless quantitative indicator matrix $R = (r_{ij})_{m.3}$. The weighting of the decision indicators for the different inflow options is then determined using a combination of weights ω_j. The weighted Euclidean distances to the positive and negative ideal solutions d^+_i, d^-_i and the closeness of the alternatives to the ideal solution μ_i are also calculated for each alternative. The expression is given in Eq. (13):

$$\begin{cases} d_i^+ = \sqrt{\sum_{j=1}^{3} \omega_j^2 \left(r_{ij} - 1\right)^2} \\ d_i^- = \sqrt{\sum_{j=1}^{3} \omega_j^2 r_{ij}^2} \\ \mu_i = d_i^- \big/ \left(d_i^- + d_i^+\right) \end{cases} \tag{13}$$

The different alternatives are prioritised by the magnitude of the closeness obtained. The closeness indicates how close the different alternatives are to the positive ideal solution, and the larger the value obtained, the better the solution is. A schematic representation of the overall operation steps of the experiment is finally obtained in Fig. 6.

4. Performance testing and application effects of multi-objective decision models

In order to verify the effectiveness of the multi-objective decision system constructed by the study in a civil engineering flood construction risk analysis system, the study first tested the performance of the constructed system. The basic environment setup for the experiments is shown in Table 1.

The study firstly selected particle swarm modified least squares support vector machine algorithm (PSO-SVM) and ant colony algorithm (ACO) with the same experimental experience to compare the performance with the research method and experimental method in the literature [21]. Also, to ensure fairness and reasonableness in conducting the experiments, the experiments were set to 150 iterations for all algorithms. The ASCE dataset and the B-item dataset from the Guotaian dataset repository were then selected as the experimental dataset to test the performance of the model, where the convergence variation of the different algorithms is shown in Fig. 7.

Fig. 7a shows the variation of the fitness values on the ASCE dataset. As the number of training iterations increases, the fitness values of both ACO and literature [21] methods begin to zigzag, but never have a stable value; when the iteration proceeds to 90, PSO-SVM has a smooth fitness value of 93.68; while the research method has a maximum fitness value of 97.89 at the 58th iteration and stays more stable thereafter. This indicates that the convergence of the research method is more stable. Fig. 7b shows a test of the fitness values on the Project B dataset, where the number of iterations of the system increases the fitness values of the

Table 1
Experimental basic environmental parameters

Parameter variables	Parameter selection
Overall implementation platform of the system	Simulink
Operating system	Windows 10
Operating environment	MATLAB
System PC side memory	12G
CPU dominant frequency	2.62Hz
GPU	RTX-2070
Central processing unit	i7-8700
Data storage	MySQL data bank
Data regression analysis platform	SPSS 26.0

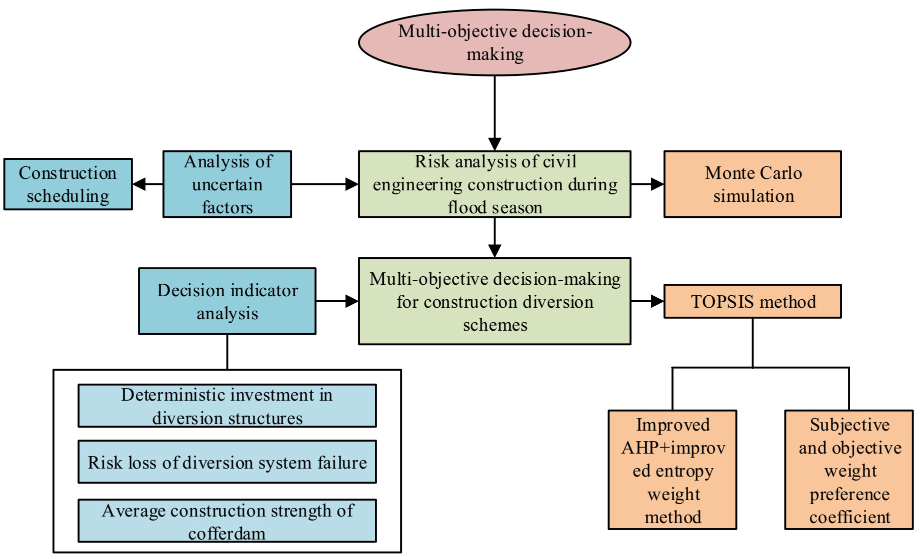

Fig. 6. Schematic representation of the overall running steps of the experiment.

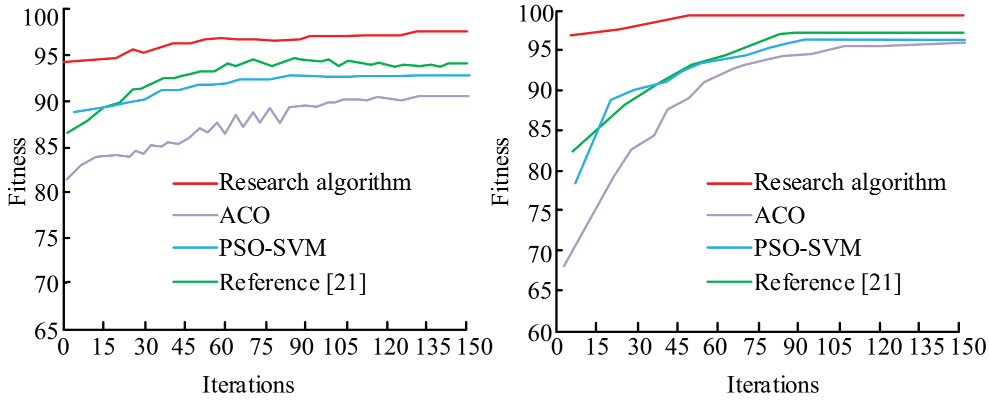

(a) ASCE dataset (b) B Project dataset

Fig. 7. Comparison of convergence variation of different algorithms.

four algorithms. The research method has the highest fitness value at 46 iterations and converges to 99.99%, while all other algorithms reach a stable fitness value after 90 iterations and are smaller than the research method. In comparison, the research method has the best fitness and achieves a stable convergence rate more quickly. The ASCE dataset was then used as the main experimental dataset to extend the experiments. the changes in the Receiver Operating Characteristic Curve (ROC) curves are shown in Fig. 8.

The area enclosed by the curves formed by the different method trends and the FP rate in Fig. 8 is the area under the ROC curve. The AUC values for the research method, PSO-SVM, ACO and the literature [21] were calculated to be 0.941, 0.923, 0.889 and 0.864, respectively, and the comparison shows that the research method has the largest area value, followed by the method in the literature [21]. This indicates that the research method performs significantly better than the other three methods and is able to provide a good analysis of the risks of civil engineering flood construction. In addition to this, the variation in the combined F1 values of the four methods for the risk analysis of data related to civil engineering construction in the two datasets is shown in Fig. 9.

As can be seen in Fig. 9, the F1 values of all the models start to rise sharply as the running time of the system increases. However, when the rise reaches a certain level, the change in F1 values starts to become smaller and tends to a steady state indefinitely. When the time reached 0.98 s, the study method gradually stabilised with an F1 value of 98.45%. While the other three methods all started to stabilise after 1.00 s. The F1 values of the research method are 0.56%, 1.20% and 0.99% higher than those of the literature [21], ACO and PSO-SVM models, respectively. The comparison shows that the research method has the highest F1 value and the model has the best accuracy performance. The squared correlation coefficients and mean squared errors of the research methods in the different data sets were then analysed and are shown in Fig. 10.

From Fig. 10a, the value of the squared correlation coefficient for the study method in the ASCE dataset is 0.9256 and the value of the mean squared error is 0.00534. The magnitude of the two values indicates that the study method has a high accuracy in the ASCE dataset. As can be seen from Fig. 10b, the squared correlation coefficient and mean squared error of the research method in the Project B dataset are 0.8827 and 0.01283, respectively. as the squared

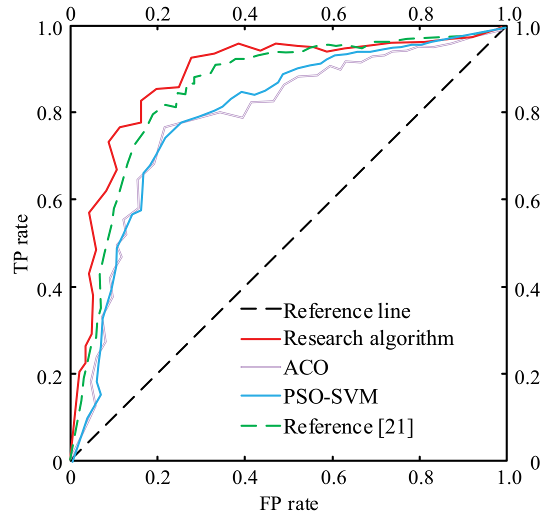

Fig. 8. Comparison of ROC curves of different algorithms.

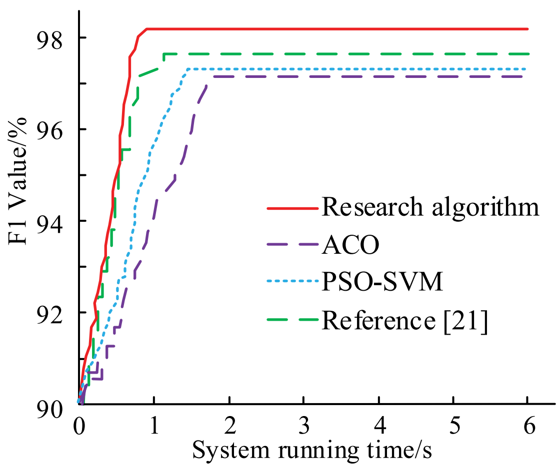

Fig. 9. The F1 values for the different models.

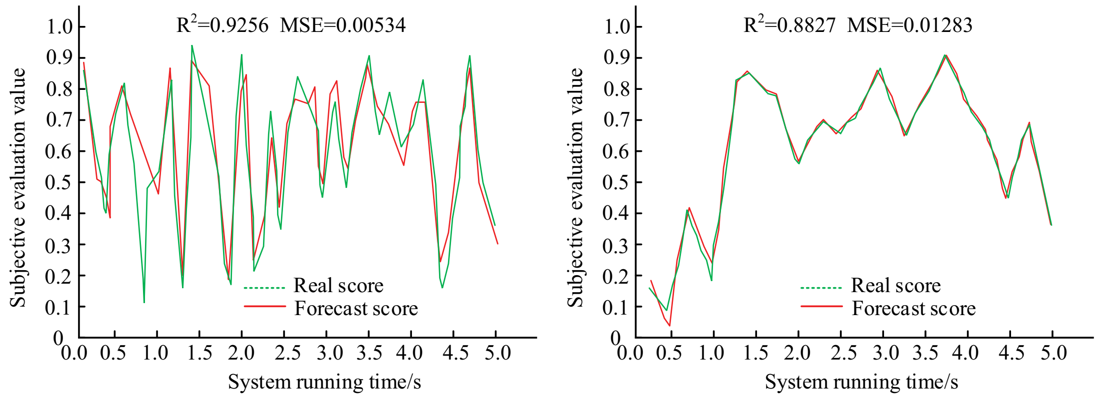

(a) ASCE dataset (b) B Project dataset

Fig. 10. Squared correlation coefficients and mean squared errors for different models.

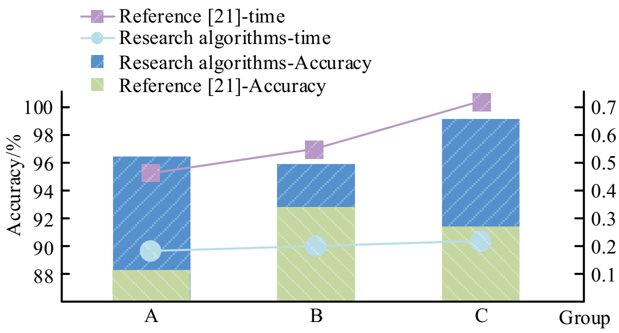

Fig. 11. Accuracy of risk analysis by different methods vs. system running time.

relative coefficient values are both greater than 0.90, this indicates a strong generalisation capability of the research method. Finally, using a reservoir construction project as an application example, the multi-objective decision model constructed by the study and the research method in the literature [21] were used to test the application of construction inflow during the civil engineering construction flood period, and then to verify the feasibility and reasonableness of the model in the actual engineering construction. Three sets of experiments were carried out with test time and test accuracy as variables. The specific results obtained are shown in Fig. 11.

As can be seen in Fig. 11, in group A experiments, the inflow accuracy of the study method in the literature [21] was 88.256% with a run time of 0.489 s. In group B experiments, the inflow accuracy of the study method in the literature [21] was 92.584% with a run time of 0.523 s. The inflow accuracy of the study in group C, the inflow accuracy of the method in the literature [21] was 91.773% with a running time of 0.715 s. The inflow accuracy of the method in the literature [21] was 99.869% with a running time of 0.211 s. Comparing the data from the three experimental groups, it can be found that the inflow accuracy of the research method in groups A and C was the best infusion results were achieved in groups A and C, with an accuracy of over 96%. The small variation in the run time of the research method in the three sets of experiments indicates that the research method is able to develop a reasonable construction diversion plan for the actual construction of the project during the flood season, while reducing the analysis time and effectively avoiding risks.

5. Conclusion

The construction period is a high risk period for dam failure and plays an important role in the control of civil engineering risks. A mathematical model of flood risk was constructed using the probability of dam failure as an indicator of the degree of flood risk during the construction phase of a civil engineering project. This model was used as a basis for making effective decisions on the construction of diversion schemes in civil engineering construction by selecting the deterministic investment in diversion buildings, the risk of failure of the diversion system and the average construction intensity of the diversion buildings, and using TOPSIS to achieve multi-objective decision-making. The results show that the PSO-SVM has a smooth adaptation value of 93.68 at 90 iterations in the Project B dataset, while the research method has a maximum adaptation value of 97.89 at the 58th iteration and remains relatively stable thereafter. This indicates that the convergence of the research method is more stable. The area under the ROC curve is 0.941, 0.923 and 0.889 for the research method, PSO-SVM and ACO, respectively, indicating that the research method has the largest area value and can provide a good analysis of the risk of civil engineering flood construction. Also, in the ASCE dataset, the value of the study squared correlation coefficient is 0.9256 and the value of the mean squared error is 0.00534, which has a high accuracy. In the comparison of the three sets of experimental data, the study method has the best inflow effect with an accuracy of over 96% in all cases, proving the effectiveness of the method in flood risk planning. However, the decision indicators selected for the study are all easily quantifiable in practical engineering and may have certain deviations. It is necessary to consider the decision methods under different types of diversion buildings in the future in order to obtain a solution that better meets the needs of practical engineering.

Fundings

This research was supported by Henan Provincial Department of Education 2024 Key Scientific research of Universities in Henan Province Promotion and Application of Rural Prefabricated Building Technology under the Background of Rural Revitalization (No. 24B560018).

References

[1] D.J. Bandyopadhyay, D. Karar, Modeling fire station establishment of industrial area using geo-spatial science, Knowledge-Based Eng. Sci., 4 (2023) 19–36.
[2] Y. Wang, Y. Liu, W. Feng, S. Zeng, Waste haven transfer and poverty-environment trap: evidence from EU, Green Low-Carbon Econ., 1 (2023) 41–49.
[3] M. Barma, U.M. Modibbo, Multiobjective mathematical optimization model for municipal solid waste management with economic analysis of reuse/recycling recovered waste materials, J. Comput. Cognit. Eng, 1 (2022) 122–137.
[4] I. Sahmutoglu, A. Taskin, E. Ayyildiz, Assembly area risk assessment methodology for post-flood evacuation by integrated neutrosophic AHP-CODAS, Nat. Hazards, 116 (2023) 1071–1103.
[5] K. Jain, A. Saxena, Simulation on supplier side bidding strategy at day-ahead electricity market using ant lion optimizer, J. Comput. Cognit. Eng, 2 (2022) 17–27.
[6] J. Li, J. Huang, P. Liang, J.R. Lund, Fuzzy representation of environmental flow in multi-objective risk analysis of reservoir operation, Water Resour. Manage., 35 (2021) 2845–2861.
[7] S. Bao, Z. Lai, B. Chen, S. Chen, Urban drainage decision model for storm emergency management based on multi-objective optimization, Stochastic Environ. Res. Risk Assess., 37 (2023) 813–829.
[8] W. He, W. Li, S. Xu, A Lyapunov drift-plus-penalty-based multi-objective optimization of energy consumption, construction period and benefit, KSCE J. Civ. Eng., 24 (2020) 2876–2889.
[9] Z. Feng, W. Niu, C. Cheng, J. Zhou, T. Yang, China's hydropower energy system toward carbon neutrality, Front. Eng. Manage., 9 (2022) 677–682.
[10] B. Nematollahi, M.R. Nikoo, A.H. Gandomi, N. Talebbeydokhti, G.R. Rakhshandehroo, A multi-criteria decision-making optimization model for flood management in reservoirs, Water Resour. Manage., 36 (2022) 4933–4949.
[11] X. Wu, Z. Wang, Multi-objective optimal allocation of regional water resources based on slime mould algorithm, J. Supercomput., 78 (2022) 18288–18317.
[12] A. Mohanavelu, B.-S. Soundharajan, O. Kisi, Modeling multi-objective Pareto-optimal reservoir operation policies using state-of-the-art modeling techniques, Water Resour. Manage., 36 (2022) 3107–3128.
[13] W.J. Raseman, J.R. Kasprzyk, R. Scott Summers, A.K. Hohner, F.L. Rosario-Ortiz, Multi-objective optimization of water treatment operations for disinfection byproduct control, Environ. Sci.: Water Res. Technol., 6 (2020) 702–714.
[14] U.M. Modibbo, I. Ali, A. Ahmed, Multi-objective optimization modelling for analysing sustainable development goals of Nigeria: Agenda 2030, Environ. Dev. Sustainability, 23 (2021) 9529–9563.
[15] N. Elshaboury, Prioritizing risk events of a large hydroelectric project using fuzzy analytic hierarchy process, J. Project Manage., 6 (2021) 107–120.
[16] H.A. Yazbek, F. Surriya, S.U. Khan, N. Jan, D. Marinkovic, A novel approach to model the economic characteristics of an organization by interval-valued complex Pythagorean fuzzy information, J. Comput. Cognit. Eng., 2 (2023) 75–87.
[17] Z. Wu, Y. Zhao, N. Zhang, A literature survey of green and low-carbon economics using natural experiment approaches in top field journal, Green Low-Carbon Econ., 1 (2023) 2–14.
[18] S. Bucking, M. Rostami, J. Reinhart, M. St-Jacques, On modelling of resiliency events using building performance simulation: a multi-objective approach, J. Build. Perform. Simul., 15 (2022) 307–322.
[19] E. Nsugbe, Toward a self-supervised architecture for semen quality prediction using environmental and lifestyle factors, Artif. Intell. Appl., 1 (2023) 35–42.
[20] M.M.R. Tabari, R. Safari, Development of water re-allocation policy under uncertainty conditions in the inflow to reservoir and demands parameters: a case study of Karaj AmirKabir dam, Soft Comput., 27 (2023) 6521–6547.
[21] S.M. Jafari, A. Zahiri, O. Bozorg-Haddad, M.M.R. Tabari, Development of multi-objective optimization model for water distribution network using a new reliability index, Int. J. Environ. Sci. Technol., 19 (2022) 9757–9774.